THE JOURNAL OF BIOLOGICAL CHEMISTRY VOL. 286, NO. 40, pp. 35196–35208, October 7, 2011

Recycling of the Epidermal Growth Factor Receptor Is Mediated by a Novel Form of the Clathrin Adaptor Protein Eps15*[S]

Received for publication, April 4, 2011, and in revised form, August 1, 2011 Published, JBC Papers in Press, August 8, 2011, DOI 10.1074/jbc.M111.247577

Susan Chi, Hong Cao, Yu Wang, and Mark A. McNiven[1]

From the Department of Biochemistry and Molecular Biology and Center for Basic Research in Digestive Diseases, Mayo Clinic, Rochester, Minnesota 55905

Background: Sorting of EGFR is tightly regulated by the endocytic machinery.
Results: Disruption of a new isoform of Eps15 function inhibits EGFR recycling.
Conclusion: A novel form of Eps15, Eps15S, regulates EGFR recycling and function of the ERC.
Significance: This finding suggests that distinct forms of Eps15 can function differentially in EGFR trafficking.

Levels of the epidermal growth factor receptor (EGFR) at the cell surface are tightly regulated by a complex endocytic machinery. Following internalization, EGFR is either recycled back to the cell surface or transported to the late endosome/lysosome for degradation. Currently, the molecular machinery that regulates this sorting pathway is only partially defined. Eps15 (EGFR pathway substrate 15) is an endocytic adaptor protein that is well known to support clathrin-mediated internalization of EGFR at the plasma membrane. Using RT-PCR, we have identified a novel short form of Eps15 (Eps15S) from rat liver that lacks the 111 C-terminal amino acids present in the traditional Eps15 form. The goal of this study was to define the functional role of the novel Eps15S form in EGFR trafficking. Overexpression of a mutant form of Eps15S (Eps15S ΔEH2/EH3) did not block EGFR internalization but reduced its recycling to the cell surface. After knockdown of all Eps15 forms, re-expression of Eps15S significantly reduced EGFR degradation while promoting recycling back to the cell surface. In contrast, re-expression of Eps15 did not potentiate receptor recycling. Furthermore, overexpression of the mutant Eps15S substantially reduced cell proliferation, linking EGFR recycling to downstream mitogenic effects. Finally, we found that Eps15S is localized to the Rab11-positive recycling endosome that is disrupted in cells expressing the Eps15S mutant, leading to an accumulation of the EGFR in early endosomes. These findings suggest that distinct forms of Eps15 direct EGFR to either the late endosome/lysosome for degradation (Eps15) or to the recycling endosome for transit back to the cell surface (Eps15S).

Endocytosis and endosomal sorting of plasma membrane proteins play a key role in the regulation of multiple cellular processes, including signaling cascades, mitotic growth, and cell migration. Receptor signaling relies on a delicate balance. On the one hand, endocytic internalization and subsequent trafficking to the lysosome promotes degradation and the attenuation of signaling; and on the other hand, prolonged retention in a signaling endosomal compartment allows recycling back to the plasma membrane (1–3). A central goal in receptor biology is to define the cellular mechanisms that influence this sorting switch. One of the best understood of these targeting mechanisms is the ligand-induced ubiquitination of the EGFR[2] tail that protrudes from the lumen of the nascent endosome into the cytoplasm. This modification is recognized by the endosomal sorting complex required for transport (ESCRT) machinery, which facilitates transit through the late endosome to the lysosome (4–6). Importantly, the concentration of EGF ligand can influence the level of receptor ubiquitination and alter the balance between the lysosomal degradation and recycling pathways (7). Numerous components of this recycling pathway have been identified in recent years, including the Rab and Arf GTPases and Eps15 homology (EH) domain-containing proteins (2, 8–10). Rab4 and Rab35 have been described as important regulators of direct recycling from the early endosome to the cell surface (11–13). Rab11 and Rab11 family interacting proteins (Rab11FIPs) support indirect recycling from the early endosome to the endocytic recycling compartment (ERC) and subsequently to the plasma membrane, whereas Arf6 and EH domain-containing proteins regulate both the perinuclear positioning of the ERC and cargo transport (8, 12, 14–18).

Because EGFR and other receptor tyrosine kinases require phosphorylation and subsequent ubiquitin modification for targeting to the lysosome, one could infer that endocytosed cargo that is recycled back to the plasma membrane is missing these molecular tags. Whether recycling is truly a "default" pathway remains unclear, making it important to fully define the adaptors and sorting machinery that provide this essential

* This study was supported by Grants R01 DK44650 (to M. A. M.) and P30DK84567 from the Optical Core of the Mayo Clinic Center for Cell Signaling in Gastroenterology.
[S] The on-line version of this article (available at http://www.jbc.org) contains supplemental Figs. 1 and 2.
[1] To whom correspondence should be addressed: Dept. of Biochemistry and Molecular Biology, Guggenheim 1637, Mayo Clinic, 200 First St. SW, Rochester, MN 55905. Tel.: 507-284-0683; Fax: 507-284-2053; E-mail: mcniven.mark@mayo.edu.

[2] The abbreviations used are: EGFR, epidermal growth factor receptor; TfR, transferrin receptor; EH, Eps15 homology; ERC, endocytic recycling compartment; UIM, ubiquitin-interacting motif; HBSS, Hanks' balanced salt solution; RF, rat fibroblast; Rh-EGF, rhodamine-tagged EGF.

ferreting function. One such adaptor is the EGFR pathway substrate 15 (Eps15), which is well known to function in endocytosis at the plasma membrane and in downstream trafficking (19–22). Eps15 possesses several interactive structural domains, most notably three N-terminal EH domains that mediate binding to the asparagine-proline-phenylalanine (NPF) motifs of epsin and synaptojanin (23, 24). Disruption of the second and third EH domains inhibits the internalization of transferrin and EGF (19, 20). Furthermore, multiple aspartate-proline-phenylalanine (DPF) motifs near the C terminus of Eps15 facilitate an interaction with AP-2 at the rims of clathrin-coated pits (20, 25, 26). Two ubiquitin-interacting motifs (UIMs) at the very C terminus are necessary for intra- and intermolecular interactions with ubiquitin and have been implicated in mediating the interaction of Eps15 with ubiquitinated EGFR (27–31).

Recently, Roxrud *et al.* (32) utilized a data base search to identify a novel spliced variant of Eps15 that they termed Eps15b. Compared with conventional Eps15, this form lacks three N-terminal EH domains. Eps15b localizes at microdomains of the early endosome that contain Hrs, a key component of the ESCRT-0 complex, and interacts specifically with Hrs. Depletion of Eps15b but not Eps15 delays degradation of EGFR independently of endocytosis. Furthermore, re-expression of Eps15b but not Eps15 rescues impaired EGFR degradation in Eps15/Eps15b-depleted cells, suggesting that Eps15b complexed with Hrs is important for sorting EGFR from the early endosome for degradation. In this study, we report the identification of a new isoform of Eps15 that we refer to as Eps15 short (Eps15S) because it is missing the 111 C-terminal amino acids of Eps15, including the UIMs. Importantly, this novel form displays a distribution that differs from the other two Eps15 forms, and it appears to play a role in directing internalized EGFR back to the cell surface via the Rab11-positive ERC. These findings suggest that the Eps15 family can act at a variety of cellular locations to regulate endocytic trafficking of EGFR and cell growth.

EXPERIMENTAL PROCEDURES

Plasmid Constructs and siRNA—To identify novel Eps15-spliced forms, RT-PCR was performed from rat liver using specific primers for Eps15 as described previously (33). After PCR amplification, the reaction products were ligated into a TA vector (pCR3.1) (Invitrogen). By sequencing the ligated products, the Eps15S form was identified, with a 185-nucleotide deletion (2363–2547) at the C terminus compared with Eps15 (2694 nucleotides). The deletion caused a reading frameshift that produced a new stop codon. As a result, the Eps15S protein lacks 111 amino acids, and the three amino acids before the stop codon differ from Eps15. The Eps15S insert in a pCR3.1 vector was subcloned into the pCDNA3.1/Myc-His vector (Invitrogen).

Production of wild-type Myc-Eps15 and Myc-Eps15 ΔEH2/EH3 was described previously (33, 34). Myc-Eps15S ΔEH2/EH3 was generated in the same way as Myc-Eps15 ΔEH2/EH3 (33, 34). Full-length rat Eps15b was amplified by PCR using rat brain cDNA as a template and the following primers: 5′-AGAGGGTAGAAAAATCTGCCCTTC-3′ (forward) and 5′-TACCTGCTGTTTCTGGGCCTGT-3′ (reverse). The Eps15b insert was subsequently cloned into a pCDNA3.1/Myc-His vector. GFP-Rab11 and GFP-Rab5 were kindly provided by Dr. Richard Pagano and Dr. Bruce Horazdovsky (Mayo Clinic, Rochester, MN), respectively. GFP-Rab11^{Q70L} and GFP-Rab5^{Q79L} were generated by using PCR-based site-directed mutagenesis and verified by sequencing. GFP-EGFR was described previously (35).

A small interfering RNA (siRNA) pool targeted to the coiled-coil domain of three human Eps15 forms (Eps15, Eps15S, and Eps15b) and a nontargeting siRNA pool were purchased from Dharmacon Research (Boulder, CO). The sense sequence of the Eps15-specific siRNA was 5′-AAACGGAGCUACAGAUUAU-3′ (catalog no. D-004005-03).

Cell Culture and Transfection—HuH-7 (human hepatocellular carcinoma) and HeLa cells were maintained in minimum Eagle's medium supplemented with 10% FBS, 1 mM sodium pyruvate, 1 mM nonessential amino acids, 1.5 g/liter sodium bicarbonate, 100 units/ml penicillin, and 100 μg/ml streptomycin. Rat fibroblasts (ATCC CTL-1213; Manassas, VA) were maintained in DMEM supplemented with 10% FBS, 100 units/ml penicillin, and 100 μg/ml streptomycin. Clone 9 cells, an epithelial cell line isolated from normal rat liver (ATCC CRL-1439; Manassas, VA), were maintained in Ham's F-12K supplemented with 10% FBS, 100 units/ml penicillin, and 100 μg/ml streptomycin. Cells were transiently transfected using the Lipofectamine Plus Reagent kit according to the manufacturer's protocol (Invitrogen). Transfection of HeLa cells with siRNA was performed using RNAiMAX as specified by the manufacturer's protocol (Invitrogen).

Antibodies—Two anti-Eps15 polyclonal antibodies, the Eps15 C-terminal antibody and the Eps15 Pan antibody, were described previously (34). The polyclonal anti-Eps15 Pan (SC) antibody was obtained from Santa Cruz Biotechnology Inc. The polyclonal anti-Eps15R antibody was a kind gift from Dr. P. Di Fiore (Istituto FIRC di Oncologia Molecolare, Italy). The transferrin receptor antibody (TfR1-C) was described previously (36). The polyclonal anti-Myc antibody was purchased from Cell Signaling Technology, Inc. The monoclonal anti-EGFR antibody used for immunofluorescence and the polyclonal anti-EGFR antibody used for immunoblotting were obtained from Sigma and Cell Signaling Technology, respectively. The monoclonal anti-EEA1 antibody was purchased from BD Transduction Laboratories.

Immunoprecipitation—Lysate from rat brain or liver was incubated with the anti-Eps15 C-terminal, anti-Eps15 Pan, or anti-Eps15R antibody and combined with protein A-Sepharose beads in IP buffer (20 mM Tris-HCl, pH 7.4, 150 mM NaCl, 0.5% Triton X-100, 15 mM NaF, 2 mM Na_3VO_4, and complete protease inhibitors) for 2 h at 4 °C. The beads were washed four times with IP buffer and boiled in reducing Laemmli sample buffer. The samples were subjected to SDS-PAGE and Western blot analysis using the anti-Eps15 C-terminal, anti-Eps15 Pan, or anti-Eps15R antibody, respectively.

Immunofluorescence-based EGFR Recycling/Degradation Assays—HuH-7 cells were transfected with mock, Myc-Eps15 ΔEH2/EH3, or Myc-Eps15S ΔEH2/EH3. Cells were then serum-starved for 4 h and pretreated with 50 μg/ml cyclohex-

imide for 1 h. Cells were treated with 20 ng/ml EGF for 30 min at 4 °C in the presence of cycloheximide. The cells were then shifted to 37 °C for 15 min (pulse), washed twice with HBSS, and further incubated in serum-free medium for 60 min (chase) in the presence of cycloheximide. After fixation, cells were immunostained with the anti-EGFR antibody without permeabilization to visualize only surface EGFR. Subsequently, cells were permeabilized and immunostained with anti-Myc antibody to confirm expression of the Myc-Eps15 proteins. For the assay of EGFR recycling in cells with knocked down and re-expressed Eps15 forms, HeLa cells were transfected with human siRNA targeted to the coiled-coil domain of the three known Eps15 isoforms for 48 h. These cells were subsequently transfected with rat-specific, siRNA-resistant Myc-Eps15 or Myc-Eps15S. EGFR recycling was assessed as described above.

To measure EGFR degradation, HeLa cells were treated with siRNA targeted to the coiled-coil domain of all three Eps15 isoforms for 48 h and subsequently transfected with siRNA-resistant Myc-Eps15 or Myc-Eps15S. Cells were then serum-starved for 4 h, pretreated with 50 μg/ml cycloheximide for 1 h, and incubated with 100 ng/ml EGF for 30 min at 4 °C in the presence of cycloheximide. Subsequently, cells were shifted to 37 °C for 15 min, washed twice with HBSS, and further incubated in serum-free medium for 2 h in the presence of cycloheximide. After fixation, cells were permeabilized and immunostained with the anti-EGFR and anti-Myc antibodies.

Immunofluorescence-based Assay of Transferrin Receptor (TfR) Recycling—Clone 9 cells were transfected to express Myc-Eps15 ΔEH2/EH3 or Myc-Eps15S ΔEH2/EH3 and then serum-starved for 30 min and treated 5 μg/ml of Alexa-594-conjugated transferrin for 30 min on ice. Subsequently, cells were shifted to 37 °C for 10 min (pulse), washed twice with HBSS, and further incubated in serum-free medium for 20 or 40 min (chase). To remove surface-bound transferrin, cells were acid-stripped. Following fixation, cells were permeabilized and immunostained with anti-Myc antibody to confirm expression of the Myc-Eps15 proteins. To measure TfR recycling, Clone 9 cells were treated as described above with the addition of 50 μg/ml cycloheximide. After fixation, cells were immunostained with the anti-TfR antibody without permeabilization to visualize only surface TfR. Subsequently, cells were permeabilized and immunostained with anti-Myc antibody to confirm expression of the Myc-Eps15 proteins.

Biotinylation Assay—Biochemical EGFR recycling assays in HuH-7 cells transfected with Myc-Eps15 ΔEH2/EH3 or Myc-Eps15S ΔEH2/EH3 were performed as described above. At the indicated time points, cells were transferred to 4 °C, washed with ice-cold PBS, and incubated with 0.5 mg/ml biotin (EZ-link® Sulfo-NHS-LC Biotin, Thermo Scientific) for 30 min. Subsequently, biotin was quenched with 50 mM NH_4Cl. Cells were rinsed with PBS, lysed with RIPA buffer (150 mM NaCl, 1% Nonidet P-40, 0.5% sodium deoxycholate, 0.1% SDS, 50 mM Tris, pH 8), sonicated, and centrifuged for 10 min at 14,000 rpm and 4 °C. Equal amounts of protein were added to 50 μl of streptavidin-agarose beads (Thermo Scientific), incubated overnight, washed four times in RIPA buffer, and subjected to Western blot analysis using the anti-EGFR antibody.

Cell Proliferation Assay—HeLa cells were transfected with mock, Myc-Eps15 ΔEH2/EH3, or Myc-Eps15S ΔEH2/EH3. After 6 h, cells were seeded in 6-well plates in complete (10% FBS) medium at a density of 2×10^5 cells/well. Every 24 h, cells were trypsinized and harvested, and cell numbers were measured using a hemocytometer for 4 days.

Immunofluorescence Microscopy, Image Acquisition, Quantification, and Statistical Analysis—Immunofluorescence staining was performed as described previously (37). Cells were viewed with an Axiovert 35 or 200 M microscope (Carl Zeiss, Thornwood, NY) using a ×63, 1.4 NA, oil-immersion lens. Images were acquired with an Orca II or Orca III ERG camera (Hamamatsu, Bridgewater, NJ) using IPLab (Scanalytics, Billerica, MA). Images were subsequently adjusted in Adobe Photoshop (San Jose, CA). For immunofluorescence-based quantification of EGFR or TfR recycling, all images were taken at the same exposure time and analyzed using IPLab software. Each cell was circled, and the mean immunofluorescence intensity per circled area was measured. Background fluorescence was acquired in the same way and subtracted from the values obtained for cell measurements. To quantify colocalization between Eps15 proteins and specific endocytic compartments, ImageJ software was used, and colocalization was calculated as ratio, or correlation coefficient R^2 was obtained using LSM510 software. Statistical analysis was performed using a two-tailed paired Student's t test for each sample group. p values ≤ 0.05 were considered statistically significant and are indicated in each figure.

RESULTS

Identification of Novel Eps15 Spliced Variant—Eps15 is found at a variety of cytoplasmic locations in hepatocytes and other epithelial cells (34, 38, 39). Using RT-PCR of total rat liver RNA to search for novel forms, we subsequently observed a band of 2694 nucleotides corresponding to conventional Eps15, as well as a smaller form of 2373 nucleotides. Sequencing of this short form revealed a novel truncated Eps15 missing a 111-amino acid segment at the C terminus, which was replaced with three unique residues (VSL, Fig. 1*A*). The predicted molecular mass of this novel form, referred to as Eps15S, was ~130 kDa, compared with the ~150 kDa of the conventional Eps15 form. Importantly, as a result of this C-terminal deletion, Eps15S lacked two UIMs shown to bind to ubiquitinated EGFR (28–30). In comparison with this novel Eps15S form, a recently identified Eps15 form termed Eps15b (32) lacks the three N-terminal EH domains (Fig. 1*A*) known to interact with other endocytic proteins containing NPF motifs (23, 24).

To examine the expression profiles of the distinct Eps15 forms, Western blot analysis was performed on lysates of rat tissues, including liver, brain, and spleen, as well as of cultured rat fibroblasts (RFs) transfected to express the Eps15 or Eps15S form. The blot was probed with an Eps15 Pan antibody generated to the coiled-coil domain present in all Eps15 forms (Fig. 1*A*). Eps15 antibody-reactive bands of ~150 and ~130 kDa were found in all tissues, although far more reactivity was observed in brain and liver compared with spleen. Three Eps15 bands with different molecular masses were easily detected in control RFs as follows: a major band corresponding to Eps15 at

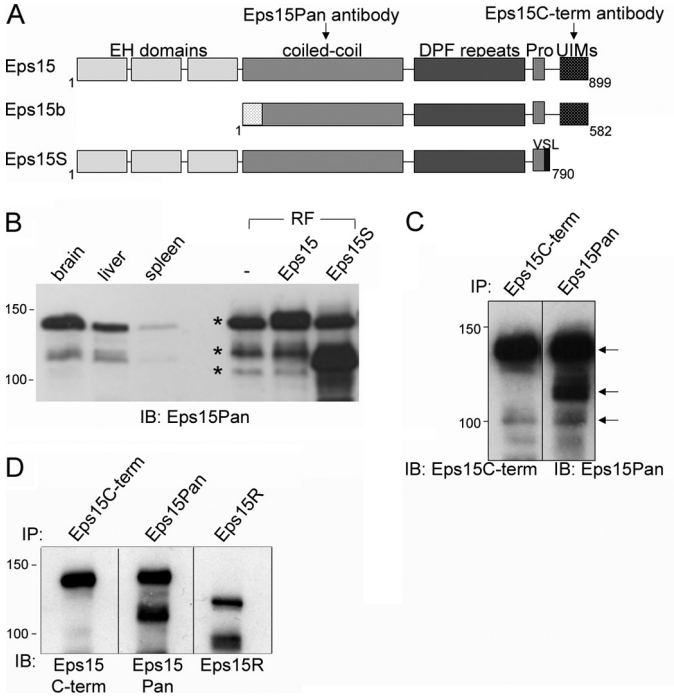

FIGURE 1. **Identification of new Eps15 short isoform Eps15S.** *A*, schematic representation of three isoforms of Eps15 as follows: conventional Eps15, Eps15b, and the newly identified Eps15S reported here. The indicated Eps15 protein domains include three Eps15 homology (*EH*) domains, a coiled-coil domain, a DPF repeat domain, a proline-rich region (*Pro*), and UIMs. The Eps15S isoform lacks the 111 amino acids at the C terminus of Eps15, including the UIMs, and has three unique amino acids (VSL) at the C-terminal (*C-term*) end. Two Eps15-specific polyclonal antibodies were generated to conserved and nonconserved domains, as indicated (*arrows*). *B,* protein extracts from rat brain, liver, and spleen or cell lysates from rat fibroblasts (*RF*) transfected with untagged Eps15 or Eps15S were subjected to SDS-PAGE and immunoblotting with the anti-Eps15Pan antibody. *Asterisks* label the three identified forms, including Eps15, Eps15S, and Eps15b, sequentially. *C,* protein extracts from rat brain were subjected to immunoprecipitation (*IP*) and immunoblotting (*IB*) using two anti-Eps15 antibodies (*Eps15 C-term* or *Eps15Pan*). *Arrows* indicate the predicted Eps15, Eps15S, and Eps15b forms. *D,* protein extracts from rat liver were subjected to immunoprecipitation and immunoblotting using three anti-Eps15 antibodies (*Eps15 C-term*, *Eps15Pan*, or *Eps15R*). Eps15 and Eps15S clearly differ from Eps15R.

~150 kDa, a second band at ~130 kDa, and a third modest protein band at ~120 kDa. Western blot analysis of exogenously expressed, untagged Eps15 and Eps15S in RFs showed an alignment of these bands with the putative endogenous forms of the proteins in the control cells and support the premise that both of these forms are normally expressed (Fig. 1*B*). The 120-kDa band likely corresponds to the Eps15b form described above. Furthermore, immunoprecipitation and Western blot analysis of the Eps15 forms from either rat brain (Fig. 1*C*) or liver (Fig. 1*D*) lysates using a novel C-terminal Eps15 UIM domain antibody or the Eps15 Pan antibody (Fig. 1*A*) revealed putative Eps15 and Eps15b bands or all three forms, respectively. Notably, the antibody to the UIM domain did not recognize the novel Eps15S form.

Because an Eps15-related protein (Eps15R) shares sequence and structural homology with Eps15 (19, 40, 41), it was important to test if the novel short form represented a distinct protein band from the Eps15R protein. Western blot analysis of immunoprecipitates from rat liver lysates using our pan- and C-terminal Eps15 antibodies, and an antibody to Eps15R, showed independent protein bands for all three forms confirming that Eps15S is a novel form of Eps15 (Fig. 1*D*). To compare the cellular distribution of the Eps15 and Eps15S forms, we utilized a cultured human hepatocyte tumor cell line (HuH-7) for immunofluorescence studies. Because all domains of the truncated Eps15S form also reside within the full-length Eps15 protein, generating a unique antibody to the novel short form was not possible. Therefore, we transiently expressed a Myc-tagged Eps15S construct to localize Eps15S. As shown in Fig. 2*A*, the expressed short form associated with numerous vesicular puncta throughout the cytoplasm. Interestingly, costaining with the Eps15 C-terminal antibody, which recognizes only the conventional Eps15 form, results in a similar punctate labeling but only modest colocalization with Myc-tagged Eps15S, suggesting that the proteins reside in distinct compartments.

To define these vesicular compartments, cells were transfected to express either form of Eps15 and then incubated with 100 ng/ml rhodamine-tagged EGF (Rh-EGF) for 15 min prior to fixation and imaging. Whereas Myc-tagged Eps15 showed strong colocalization with early endocytic vesicles containing rhodamine-EGF, as predicted by the work of others (30, 42), Myc-tagged Eps15S showed no such colocalization (Fig. 2, *B*–*B*″). To test if either Eps15 form associates with a Rab5-positive early endosomal compartment, cells were cotransfected with Eps15 or Eps15S and a GFP-tagged active $Rab5^{Q79L}$ mutant that induces large early endosomes. Cells were then fixed and viewed. As observed by Roxrud *et al.* (32), the conventional Eps15 form did not associate with $Rab5^{Q79L}$ endosomes (data not shown) nor did the Eps15S form (Fig. 2*C*′). As a positive control, cells were transfected to express the Eps15b form reported to localize with enlarged $Rab5^{Q79L}$ endosomes (32). As expected, the Myc-tagged Eps15b form localized to enlarged early endosomes (Fig. 2*C*). Taken together, our data suggest that Eps15S does not function in the early endocytic pathway.

Eps15S Participates in EGFR Recycling—The observations described above suggest that Eps15S acts in recycling of EGFR, rather than in regulating EGFR degradation like the Eps15 and Eps15b forms. To test this hypothesis, mutant constructs of Eps15 and Eps15S missing the second and third EH domains were generated. This deletion (Eps15 ΔEH2/EH3) acts as a dominant-negative protein at early steps in the endocytic pathway (20). HuH-7 cells were transfected to express either Eps15 ΔEH2/EH3 or Eps15S ΔEH2/EH3. Then the cells were serum-starved and incubated on ice with 20 ng/ml EGF for 30 min in the presence of cycloheximide. Shifting the cells to 37 °C allowed them to internalize EGFR. These cells had comparable surface EGFR levels and internalized EGFR at normal rates compared with adjacent nontransfected cells (Fig. 3, *A* and *B,* and *A*′ and *B*′). However, after a 60-min chase, cells expressing these mutants showed differential EGFR recycling rates back to the cell surface. Whereas Eps15 ΔEH2/EH3-expressing cells exhibited normal recycling of EGFR (Fig. 3*A*″), EGFR recycling was markedly reduced in cells expressing the Eps15S ΔEH2/EH3 form (Fig. 3*B*″). It should be noted that in these experiments we compared Eps15S ΔEH2/EH3 to the Eps15 ΔEH2/EH3 mutant because high levels of wild-type Eps15S expression inhibit recycling (data not shown). This effect is consistent with

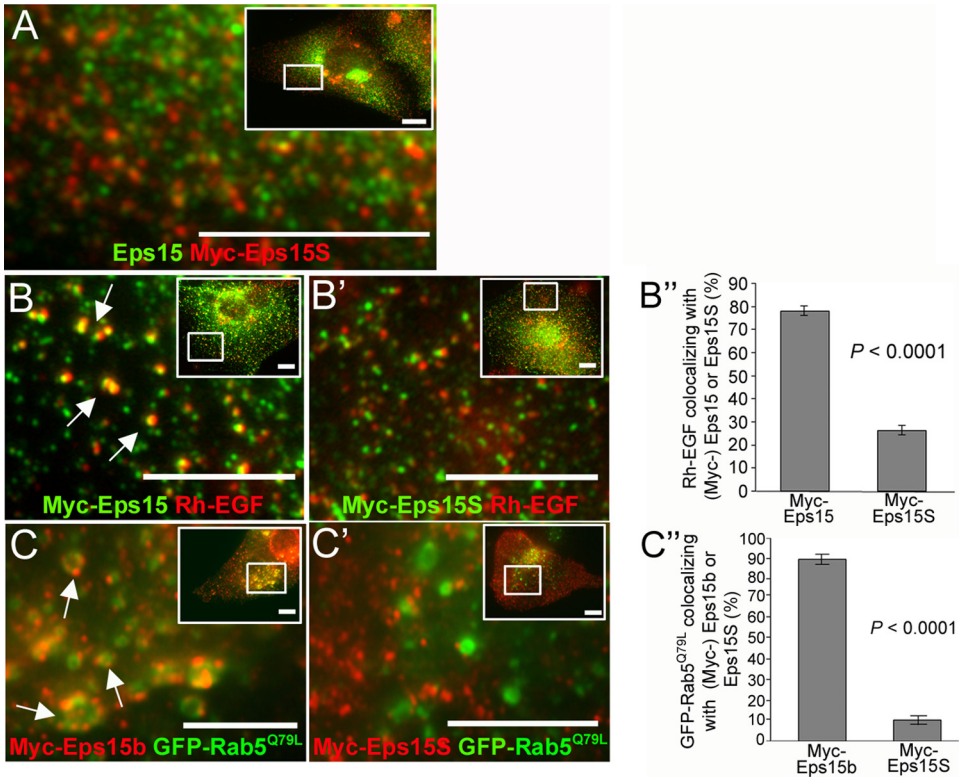

FIGURE 2. **Eps15S associates with distinct vesicle populations from Eps15 and Eps15b.** *A*, HuH-7 cells were transfected with Myc-Eps15S and immunostained for Myc (*red*) and endogenous Eps15 (*green*). Higher magnification image shows that Eps15S localizes to different regions from Eps15. *B and B′*, HuH-7 cells were transfected with Myc-Eps15 (*B*) or Myc-Eps15S (*B′*). Cells were then incubated with Rh-EGF (100 ng/ml, *red*) for 15 min and immunostained for Myc (*green*). Higher magnification images of *boxed regions* show that Myc-Eps15, but not Myc-Eps15S, colocalized with internalizing Rh-EGF (*B, arrows*). *B″*, quantitation of the amount of Rh-EGF colocalizing with Myc-Eps15 or Myc-Eps15S. For each condition, ≥15 cells were measured. Rh-EGF colocalization with Myc-Eps15 is significantly higher than with Myc-Eps15S ($p < 0.0001$). *C* and *C′*, HuH-7 cells were transfected with Myc-Eps15b (*C*) or Myc-Eps15S (*C′*) and with constitutively active Rab5 (GFP-Rab5^{Q79L}) to induce an enlargement of early endosomes (*green*). Cells were then immunostained for Myc (*red*). Higher magnification images show that Myc-Eps15b, but not Myc-Eps15S, localized on the enlarged early endosome of GFP-Rab5^{Q79L} (*C, arrows*). *C″*, quantitation of GFP-Rab5^{Q79L}-positive early endosomes colocalizing with Myc-Eps15b or Myc-Eps15S. For each condition, ≥30 cells were measured. Significantly more GFP-Rab5^{Q79L} colocalizes with Myc-Eps15b than Myc-Eps15S ($p < 0.0001$). *Error bars* indicate standard error. *Scale bars,* 10 μm.

that observed by others expressing Eps15b (32). Quantitation of the fluorescence intensity of EGFR on the cell surface showed that EGFR in Eps15S ΔEH2/EH3-expressing cells did not recycle to the cell surface, although EGFR in the Eps15 mutant cells recycled at levels equal to mock-transfected cells (Fig. 3*C*).

These morphological experiments suggest that the Eps15S form participates in endocytic recycling, although the conventional Eps15 form does not. To extend these observations using a biotinylation approach, HuH-7 cells were transfected to express EH truncation mutants and then treated with 20 ng/ml EGF as described above. Cells were incubated on ice with biotin to label cell surface proteins. Biotinylated cell surface proteins were precipitated using streptavidin-agarose beads, and Western blot analysis was performed with the EGFR antibody. As shown in Fig. 3*D*, levels of EGFR on the surface of HuH-7 cells expressing the Eps15 mutant forms decreased after the addition of 20 ng/ml ligand (15-min pulse) indicating no defect in EGFR internalization. However, a 60-min chase allowing endocytic trafficking resulted in different receptor levels at the plasma membrane compared with control (no EGF). Although the Eps15 ΔEH2/EH3-expressing cells returned over 80% of internalized receptor back to the surface, the Eps15S ΔEH2/EH3-expressing cells recycled significantly less EGFR (30%) suggesting that the two Eps15 forms perform distinct functions, and Eps15S is necessary for EGFR recycling (Fig. 3, *D* and *E*).

To further test the functional role of Eps15S in the recycling of EGFR, we utilized an RNAi approach to reduce the Eps15 levels using siRNA targeted to the coiled-coil domain of all three forms. HeLa cells were subsequently "rescue-transfected" with either WT Myc-Eps15 or Myc-Eps15S, which are siRNA-resistant because they were cloned from rat liver and contained different nucleotide sequences in the coiled-coil domain. Cells were examined for EGFR recycling. The knockdown (KD) and re-expression efficacy was greater than 95%, as confirmed by immunofluorescence staining (data not shown) and Western blot analysis (Fig. 4*A*). KD of all Eps15 forms significantly reduced EGFR recycling, even after a 60-min chase (Fig. 4). Importantly, re-expression of WT Myc-Eps15 increased the levels of EGFR recycling back to the cell surface only modestly in KD cells (Fig. 4, *B′* and *B″*), whereas cells re-expressing Myc-Eps15S exhibited a substantial (2-fold) increase in receptor recycling (Fig. 4, *C–C″* and *D*). As mentioned earlier, because of the inhibitory effects of high Eps15S expression, we needed to select cells expressing moderate levels of Eps15 or Eps15S for these experiments.

It has been well documented that high concentrations of EGF amplify EGFR phosphorylation and ubiquitination, thereby

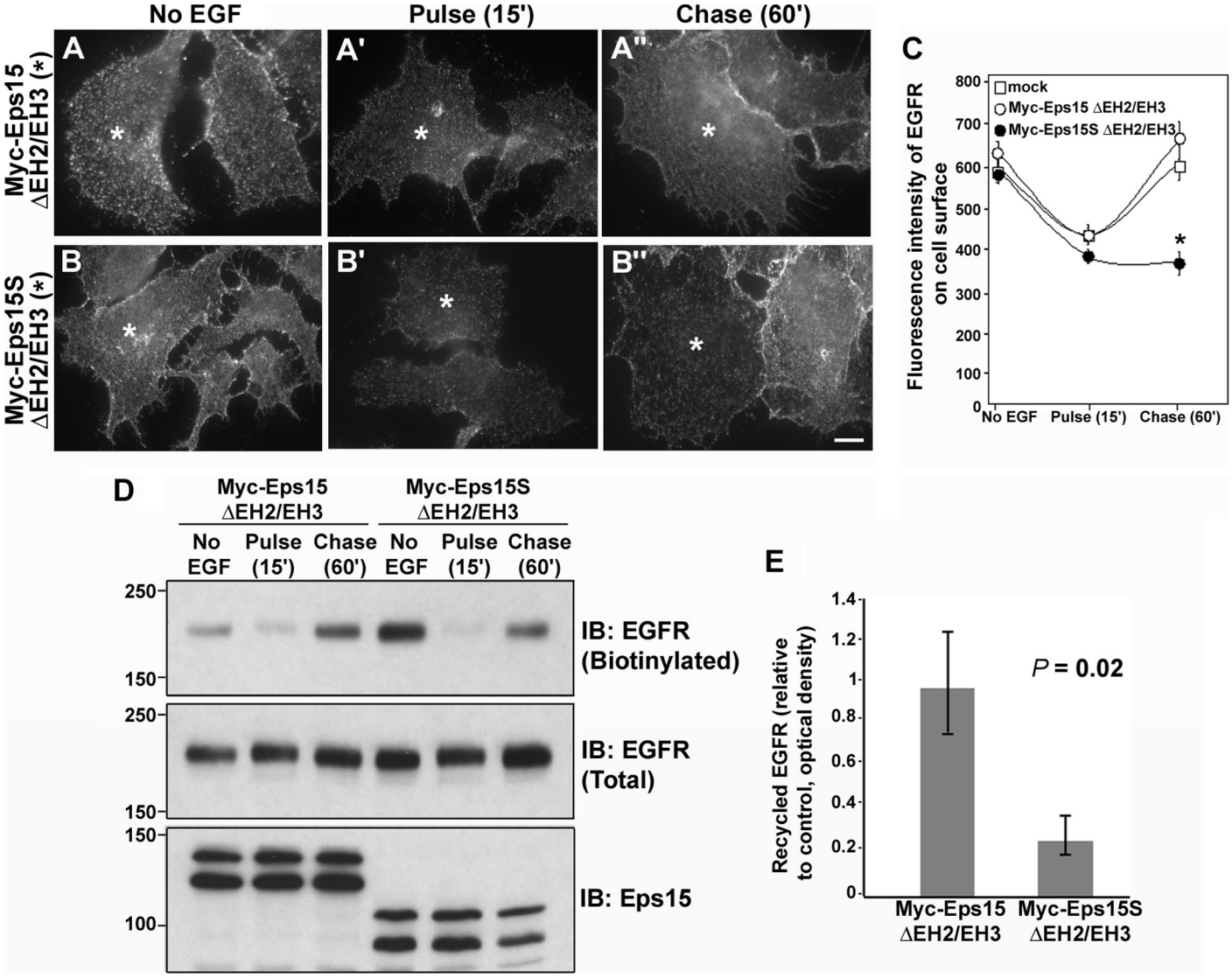

FIGURE 3. **Overexpression of a mutant Eps15S specifically blocks recycling of EGFR to the cell surface.** *A–B″*, HuH7-cells were transfected with either Myc-Eps15 ΔEH2/EH3 (*A–A″*) or Myc-Eps15S ΔEH2/EH3 (*B–B″*). Cells were then serum-starved for 4 h (*A* and *B*) and pretreated with cycloheximide for 1 h. EGF (20 ng/ml) binding occurred for 30 min at 4 °C in the presence of cycloheximide. Subsequently, cells were shifted to 37 °C for 15 min (pulse 15 min, *A′* and *B′*), washed twice with HBSS, and further incubated in serum-free medium for 60 min (chase 60′, *A″* and *B″*). After fixation, cells were immunostained for EGFR without permeabilization to visualize only surface EGFR (EGFR recycling). Subsequently, cells were permeabilized and immunostained for Myc to confirm expression of the Myc-Eps15 proteins (*). EGFR internalization was not reduced in cells expressing either Myc-Eps15 ΔEH2/EH3 or Myc-Eps15S ΔEH2/EH3 (* in *A′* and *B′*). However, recycling of EGFR to the cell surface was reduced significantly in Myc-Eps15S ΔEH2/EH3-expressing cells (* in *B″*) but not in Myc-Eps15 ΔEH2/EH3-expressing cells (* in *A″*). *C*, quantitation of the average fluorescence intensity of EGFR at the cell surface at the indicated time points. Forty cells were measured for each condition. Overexpression of Myc-Eps15S ΔEH2/EH3 caused a significant delay in EGFR recycling to the cell surface (*, $p < 0.0001$), whereas Myc-Eps15 ΔEH2/EH3 did not affect EGFR recycling. *Error bars* indicate the standard error. *Scale bars,* 10 μm (*A–B″*). *D*, HuH-7 cells were subjected to a surface biotinylation assay, and immunoblotting (*IB*) was performed using an anti-EGFR antibody to detect surface EGFR (biotinylated EGFR). Less surface EGFR was detected after the 60-min chase in Eps15S ΔEH2/EH3-expressing cells compared with Eps15 ΔEH2/EH3-expressing cells. *E*, ratio of recycled EGFR determined from densitometry of Western blot bands from three independent experiments. Biotinylated EGFR after the 60-min chase was normalized to total EGFR and then divided by biotinylated, normalized EGFR at the control time point. The level of recycled EGFR is significantly less in Myc-Eps15S ΔEH2/EH3-expressing cells compared with Myc-Eps15 ΔEH2/EH3-expressing cells ($p = 0.02$). *Error bars* indicate standard error.

promoting trafficking of this receptor to the lysosome for degradation rather than recycling (7, 30, 43). Based on this premise, we tested if modest re-expression of the Eps15S form following siRNA knockdown might increase receptor recycling away from the lysosome even under high concentrations of agonist. If so, we would expect higher total cellular levels of EGFR in these rescued cells because of reduced EGFR degradation, with a large portion residing on the cell surface. As shown in Fig. 5*A*, re-expression of the conventional Eps15 form in the KD cells treated with 100 ng/ml EGF did not increase total EGFR levels compared with adjacent untransfected cells, suggesting that the degradative pathway was not attenuated. In contrast, cells re-expressing Eps15S retained significantly higher total EGFR levels compared with adjacent cells (Fig. 5*B*). A substantial portion of this increased receptor level appears to be recycled to the plasma membrane as staining of surface EGFR with nonpermeabilized cells showed increased level of the receptor in transfected cells (Fig. 5*C*). Quantitation of fluorescence intensity of total EGFR levels showed that EGFR degradation was markedly attenuated (4–5-fold) in stimulated Eps15 siRNA-treated *ver-*

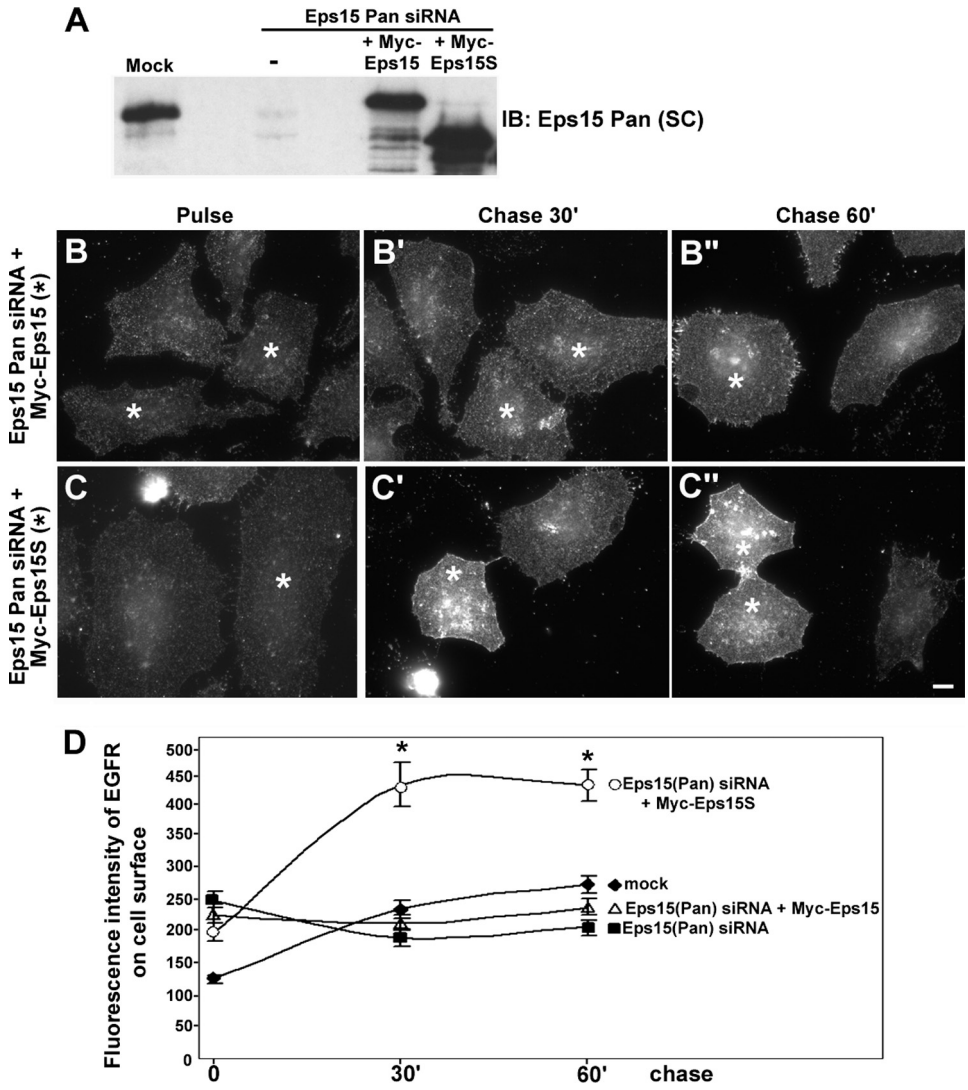

FIGURE 4. **Eps15S, but not Eps15, promotes EGFR recycling.** *A,* HeLa cells were treated with siRNA targeted to the coiled-coil domain of the three known Eps15 isoforms (*Eps15 Pan siRNA*). The cells were then transfected to re-express Myc-Eps15 or Myc-Eps15S. Cell lysates were subjected to SDS-PAGE and immunoblotting (*IB*) with the anti-Eps15Pan (*SC*) antibody. *B–C″,* HeLa cells treated with Eps15 Pan siRNA were transfected to re-express Myc-Eps15 (*B–B″*) or Myc-Eps15S (*C–C″*). EGFR recycling was assayed as described under "Experimental Procedures." Expression of either Myc-Eps15 or Myc-Eps15S was confirmed by immunostaining for Myc (data not shown). At 30 min (*B′* and *C′*) or 60 min (*B″* and *C″*) of chase following the 15-min pulse (*B* and *C*), EGFR recycling to the cell surface was minimal in cells expressing the Eps15 form (*) and was indistinguishable from untransfected adjacent cells (*B′* and *B″*). In comparison, substantial levels of EGFR were recycled back to the cell surface in Myc-Eps15S-re-expressing cells (* in *C′* and *C″*). *D,* quantitation of the average fluorescence intensity of EGFR at the cell surface at the indicated time points. Twenty five cells were measured for each condition. Statistical analysis revealed that re-expression of Myc-Eps15S WT significantly promoted EGFR recycling ($p < 0.0001$), whereas Myc-Eps15 WT had little effect on EGFR recycling. *Error bars* indicate the standard error. *Scale bars,* 10 μm (*B–C″*).

sus control cells (Fig. 5*D*). Importantly, EGFR levels remained high in Eps15S-re-expressing cells with over 90% of the receptor being trafficked to the surface. Thus, even when the degradative pathway is amplified by stimulating cells with high concentrations of ligand, receptor degradation can be completely averted in cells expressing the Eps15S form.

As manipulating the function and expression levels of the Eps15S form resulted in altered trafficking of the EGFR to the cell surface, it is likely that this could exert an effect on cell proliferation. To test this, HeLa cells were transfected to express either mutant Eps15S (Eps15S ΔEH2/EH3) or mutant Eps15 (Eps15 ΔEH2/EH3), and then cell proliferation was monitored over 4 days. HeLa cells transfected with the mutant Eps15S (Eps15S ΔEH2/EH3) exhibited substantially reduced cell growth (~3-fold) compared with mock-treated cells after 4 days (Fig. 5*E*). In comparison, overexpression of the conventional Eps15 ΔEH2/EH3 mutant form resulted in a more modest reduction in cell proliferation (1.5-fold). As these mutant-expressing cells internalize the receptor resulting in surface EGFR levels near those of control cells (Fig. 3), it is likely that other growth regulatory functions are altered in these mutant cells such as receptor signaling from an endosomal compartment.

Eps15S Influences the Localization and Structural Integrity of the Endocytic Recycling Compartment—Unlike Eps15S, both Eps15 and Eps15b have C-terminal UIM motifs (Fig. 1) and appear to function in directing EGFR to the degradative pathway (28–30, 32). From the experiments described above, we concluded that the novel Eps15S form participates in the recycling of EGFR away from the lysosomal pathway to

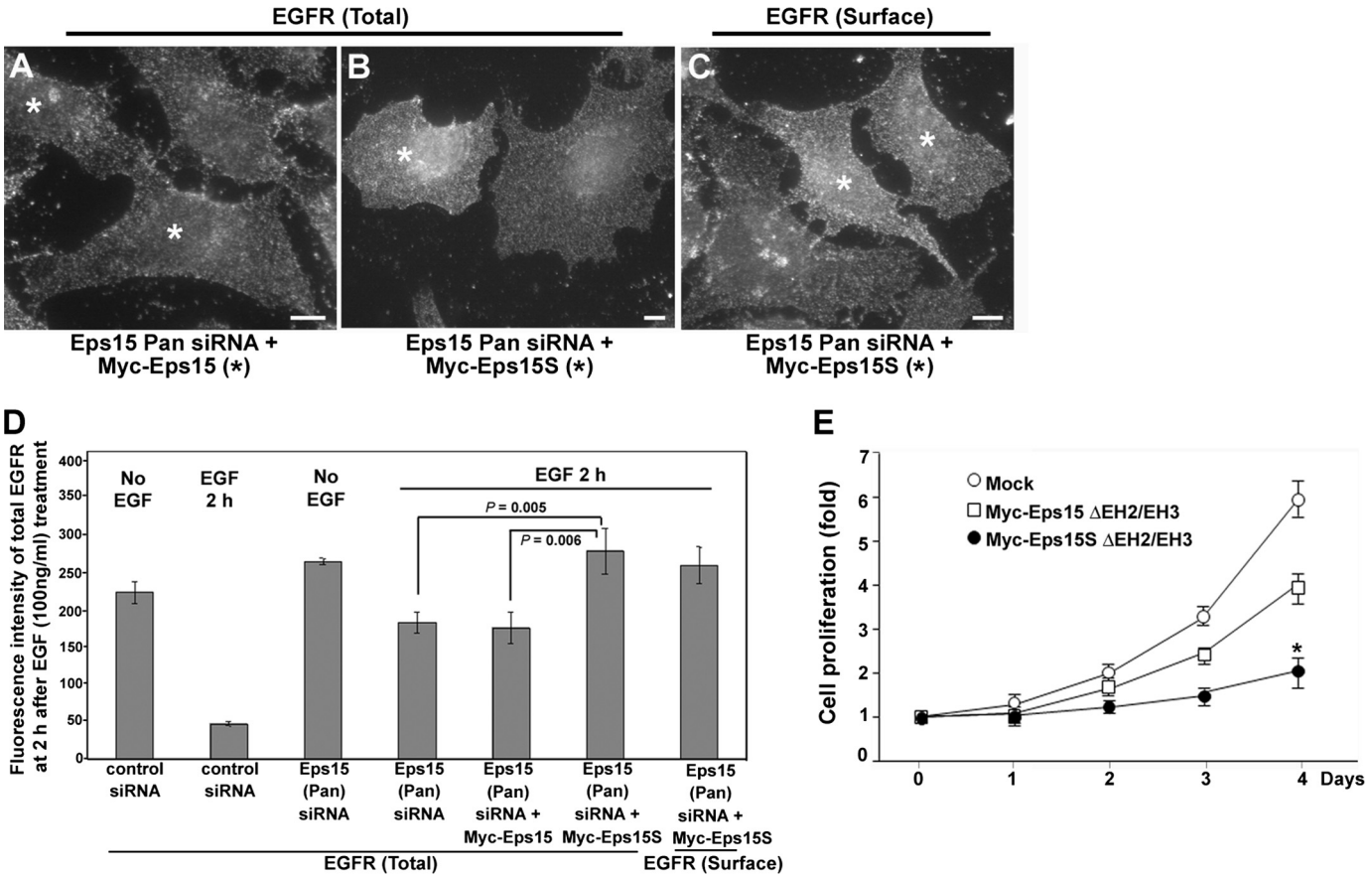

FIGURE 5. **Eps15S-expressing cells target EGFR for recycling rather than degradation.** *A–C,* HeLa cells were treated with siRNA targeted to the coiled-coil domain of three Eps15 isoforms (*Eps15 Pan siRNA*) and then transfected to re-express siRNA-resistant Myc-Eps15 (*A*) or Myc-Eps15S (*B* and *C*). Cells were serum-starved for 4 h, pretreated with cycloheximide for 1 h, and then incubated with 100 ng/ml EGF for 30 min at 4 °C in the presence of cycloheximide. Subsequently, cells were shifted to 37 °C for 15 min, washed twice with HBSS, and further incubated in serum-free medium for 2 h. After fixation, cells were permeabilized and immunostained for EGFR to examine total EGFR (*A* and *B*). To facilitate viewing of EGFR recycled back to the cell surface, cells were not permeabilized (*C*). The level of total EGFR remaining after 2 h of chase was much higher in Myc-Eps15S-re-expressing cells (* in *B*) compared with Myc-Eps15-re-expressing cells (* in *A*). Expression of Myc-Eps15 and Myc-Eps15S was confirmed by immunostaining for Myc (data not shown). *Scale bars,* 10 μm. *D,* quantitation of the average fluorescence intensity of EGFR remaining after 2 h of chase for each condition. Knockdown of all forms of Eps15 (*Eps15 Pan siRNA*) showed an ~3.5-fold higher total EGFR level after EGF treatment compared with control (*control siRNA*). Re-expression of Myc-Eps15S (*Eps15 Pan siRNA + Myc-Eps15S*), but not Myc-Eps15 (*Eps15 Pan siRNA + Myc-Eps15*), led to an even higher (~5.5-fold) level of EGFR ($p = 0.005$). A high ratio of surface EGFR to total EGFR in Myc-Eps15S-re-expressing cells indicates that Eps15S targets EGFR for recycling rather than degradation. Twenty five cells were measured for each condition. *Error bars* indicate the standard error. *E,* HeLa cells were transfected with mock, Myc-Eps15 ΔEH2/EH3, or Myc-Eps15S ΔEH2/EH3. After 6 h post-transfection, 2×10^5 of cells were plated in six wells in complete medium (10% FBS, day 0). After 24 h (day 1), cells were harvested and counted daily during 4 days. Values are expressed as a fold of control (*day 0*). The data represent the average of three independent experiments. Myc-Eps15S ΔEH2/EH3-expressing cells showed a significant delay in proliferation compared with mock-treated cells ($p = 0.002$). *Error bars* indicate the standard deviation.

the plasma membrane. The endocytic recycling endosome is an important sorting station that receives cargo from the early endosome prior to transport back to the cell surface (1, 10). This tubular-vesicular compartment resides at a perinuclear region and is regulated in part by a Rab11 GTPase (44, 45). We postulated that Eps15S, which does not reside on early endocytic vesicles or Rab5-positive early endosomes (Fig. 2), may in fact regulate the ERC. To test this prediction, HuH-7 cells were cotransfected with Myc-tagged Eps15S and GFP-tagged Rab11, a marker for the ERC. We observed a dramatic localization of Eps15S to the Rab11-positive compartment. In contrast, the Eps15 protein did not associate with the ERC (Fig. 6, *A–A″*). Expression of a constitutively active Rab11 mutant that increases the size of the ERC ($Rab11^{Q70L}$) also dramatically increased the colocalization of Eps15S but had no effect on Eps15 association (data not shown). Interestingly, removal of the UIM domain from the full-length Eps15 protein resulted in a marked increase in association between this protein and the enlarged Rab11 compartment (Fig. 6*B*), supporting the premise that the UIM domain provides important targeting information for the degradative pathway.

To test if Eps15S alters the function of the Rab11-positive compartment, wild-type Myc-Eps15S (Myc-Eps15S WT) was coexpressed with GFP-Rab11 in HuH-7 cells (Fig. 6*C*). GFP-Rab11 displayed a typical distribution to the ERC in these cells (Fig. 6*C*). However, we were surprised to find that coexpression of the Myc-Eps15S ΔEH2/EH3 mutant induced a nearly complete dispersion of the GFP-Rab11-positive compartment (Fig. 6*C′*). As shown in Fig. 6*C″*, 70% of cells expressing the Eps15S mutant displayed a dispersed ERC, compared with only 15% of cells expressing Myc-Eps15 ΔEH2/EH3. These results indicate that Eps15S governs the structural integrity and spatial distribution of the ERC and, importantly, suggest how expression of

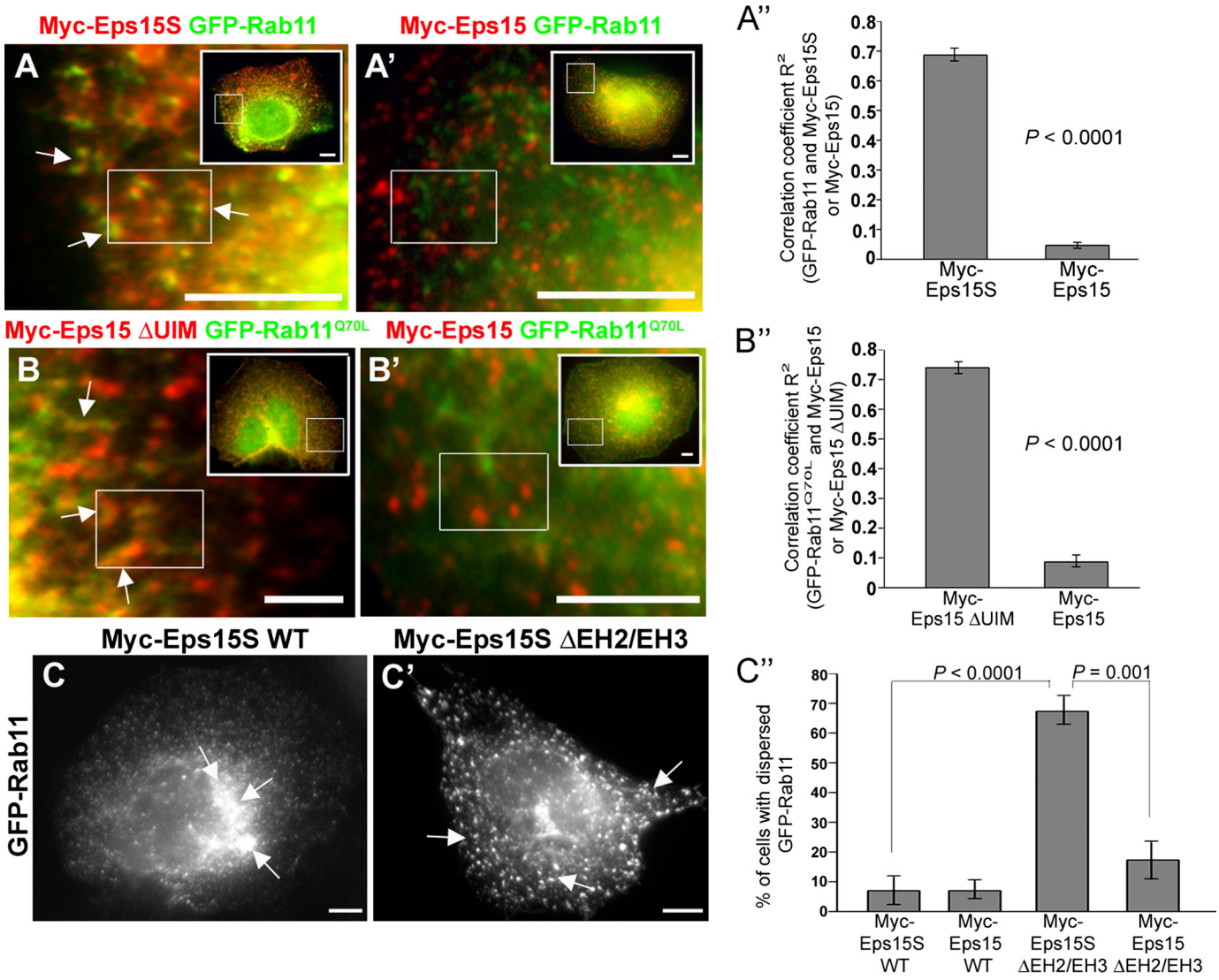

FIGURE 6. **Eps15S localizes to the Rab11-positive ERC.** *A* and *A′*, HuH-7 cells were transfected with GFP-Rab11 to label the ERC (*green*) and Myc-Eps15S (*A*) or Myc-Eps15 (*A′*). Cells were then immunostained for Myc (*red*). Higher magnification images show that only Myc-Eps15S (*A, arrows*), not Myc-Eps15 (*A′*), associates with the GFP-Rab11-positive ERC. *Scale bars,* 10 μm. *A″,* quantitation of GFP-Rab11 colocalizing with Myc-Eps15S or Myc-Eps15. Correlation coefficient R^2 between GFP-Rab11 and Myc-Eps15S or Myc-Eps15 was obtained from ≥30 random areas as shown in *boxes* drawn in each image from ≥10 cells. GFP-Rab11 colocalization with Myc-Eps15S is significantly higher than with Myc-Eps15 ($p < 0.0001$). *B* and *B′*, HuH-7 cells were transfected with constitutively active Rab11 (GFP-Rab11^{Q70L}; *green*) and Myc-Eps15 ΔUIM (*B*) or Myc-Eps15 WT (*B′*). Cells were then immunostained for Myc (*red*). Higher magnification images show that Myc-Eps15 ΔUIM (*B, arrows*), but not Myc-Eps15 WT (*B′*), colocalizes with GFP-Rab11^{Q70L}. *Scale bars,* 5 μm. *B″,* quantitation of GFP-Rab11^{Q70L} colocalizing with Myc-Eps15 ΔUIM or Myc-Eps15. A correlation coefficient R^2 between GFP-Rab11^{Q70L} and Myc-Eps15 ΔUIM or Myc-Eps15 was obtained from ≥30 random areas as shown in *boxes* drawn in each image from ≥10 cells. GFP-Rab11^{Q70L} colocalizes with Myc-Eps15 ΔUIM significantly higher than Myc-Eps15 ($p < 0.0001$). *C* and *C′*, HuH-7 cells were transfected with GFP-Rab11 and wild-type (*wt*) Myc-Eps15S (*C*) or the mutant truncated form, Myc-Eps15S ΔEH2/EH3 (*C′*). GFP-Rab11 was distributed to a condensed perinuclear localization in WT Myc-Eps15S-expressing cell (*arrows* in *C*) but appeared markedly fragmented and dispersed in Myc-Eps15S ΔEH2/EH3-expressing cells (*arrows* in *C′*). Expression levels of WT Myc-Eps15S and Myc-Eps15S ΔEH2/EH3 were confirmed by immunostaining for Myc (data not shown). *Scale bars,* 10 μm. *C″,* percentage of cells with dispersed localization of the GFP-Rab11 compartment in response to expression of the different Eps15 forms. From three independent experiments, ≥40 cells were counted for each experimental variable. Myc-Eps15S ΔEH2/EH3 induced a significant dispersion of the GFP-Rab11 compared with Myc-Eps15S WT ($p < 0.0001$) or to Myc-Eps15 ΔEH2/EH3 ($p = 0.001$). *Error bars* indicate the standard error.

this novel short mutant form disrupts recycling of the receptor back to the cell surface.

Based on the dramatic morphological changes of the Rab11-positive compartment and the recycling defect observed in cells expressing the mutant Eps15S form, the fate of the EGFR in these cells was defined. We predicted that the EGFR is either degraded by the lysosome or aberrantly retained in a compartment along the endocytic pathway. To distinguish between these two possibilities, we examined the levels and distribution of total and surface EGFR in HuH-7 cells expressing the Myc-Eps15S ΔEH2/EH3 mutant. Importantly, as shown in Fig. 7, *A* and *A′*, transfected cells exposed to a 15-min pulse with 20 ng/ml EGF followed by a 60-min chase exhibited little receptor trafficking back to the surface, yet retained substantial quantities of EGFR internally, mostly in a peri-nuclear compartment. To define the site of this intracellular retention, mutant cells expressing GFP-tagged EGFR, treated as above, were fixed and stained for a variety of endocytic marker proteins including EEA1, Rab4, and Rab7. Whereas mock-treated cells or Myc-Eps15 ΔEH2/EH3-expressing cells exhibited a colocalization

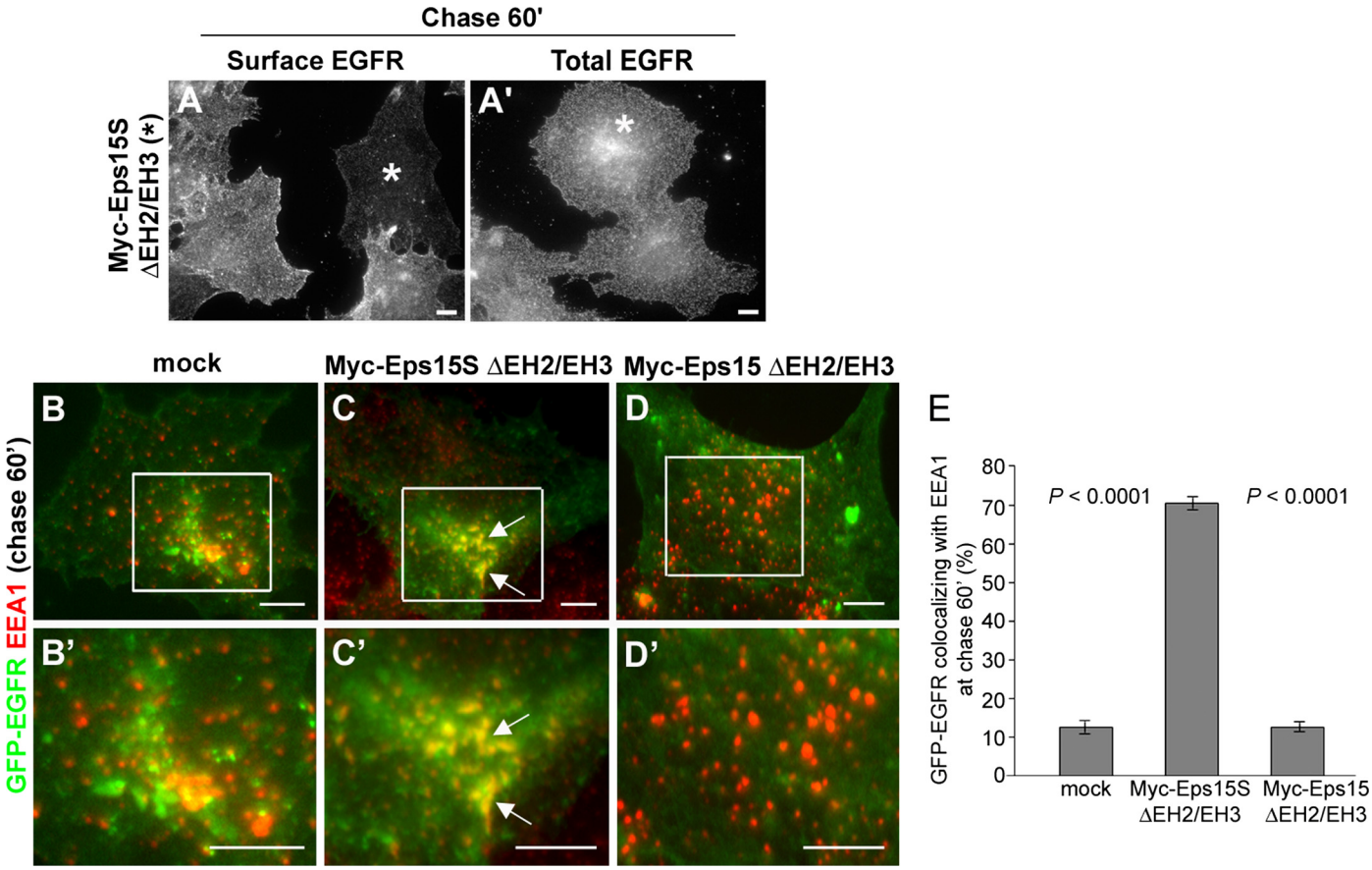

FIGURE 7. **Expression of the Eps15S ΔEH2/EH3 induces retention of EGFR in the early endosome.** *A* and *A′*, surface only (*A*) or total cellular EGFR (*A′*) following a 60-min chase with 20 ng/ml EGF was visualized as described in Fig. 5. Cells expressing the Eps15 short form mutant protein (*A*) display very modest levels of EGFR at the plasma membrane. The retained receptor in these mutant cells accumulates within a perinuclear compartment (*A′*). Expression of Myc-Eps15S ΔEH2/EH3 was confirmed by immunostaining for Myc (transfected cells indicated by *, data not shown). *B–D′*, to define the compartment to which EGFR is retained in the mutant-expressing cells, HuH-7 cells were cotransfected to express the GFP-EGFR under mock conditions (*B* and *B′*) or with Myc-Eps15S ΔEH2/EH3 (*C* and *C′*) or Myc-Eps15 ΔEH2/EH3 (*D* and *D′*). Total EGFR (GFP-EGFR; *green*) following a 60-min chase with 20 ng/ml EGF was examined as described in Fig. 5. Cells were then fixed and immunostained for EEA1 to label early endosomes (*red*). Higher magnification images of *boxed* regions show that GFP-EGFR colocalized markedly with EEA1 (*arrows* in *C* and *C′*) in Myc-Eps15S ΔEH2/EH3-expressing cells, indicating aberrant retention in the early endosome (*yellow*). Little overlap was observed in the mock (*B* and *B′*) or Eps15 mutant-expressing cells (*D* and *D′*) because EGFR was either recycled back to the cell surface or degraded. Expression of Myc-Eps15S ΔEH2/EH3 and Myc-Eps15 ΔEH2/EH3 was confirmed by immunostaining for Myc (data not shown). *E,* quantitation of GFP-EGFR colocalizing with EEA1. For each condition, ≥30 cells were measured. GFP-EGFR colocalized with EEA1 in Myc-Eps15S ΔEH2/EH3-expressing cells significantly more than in mock-treated or Myc-Eps15 ΔEH2/EH3-expressing cells ($p < 0.0001$). *Error bars* indicate standard error. *Scale bars,* 10 μm.

between EGFR and EEA1 at early time points (data not shown), by 60 min post EGF addition the receptor/ligand had trafficked past this compartment (Fig. 7, *B*, *B′*, *D,* and *D′*). Interestingly, in the Myc-Eps15S ΔEH2/EH3-expressing cells, GFP-EGFR appeared to accumulate in the EEA1-positive early endosome (Fig. 7, *C* and *C′*), suggesting that cargo is retained in the early endosome when recycling is aberrantly blocked by the Eps15S mutant protein.

Because Eps15S appears to participate in the structural maintenance and dynamics of the ERC, it seemed likely that the trafficking of other receptors could also be regulated by this adaptor. It is well known that the ERC is an important sorting compartment in transferrin receptor (TfR) trafficking (10); therefore, we tested whether the mutant Eps15S form might also have an effect on the recycling of this trophic receptor. To this end, a rat liver cell line (Clone 9) was transfected to express either Myc-Eps15S ΔEH2/EH3 or Myc-Eps15 ΔEH2/EH3. Cells were then serum-starved and incubated on ice with transferrin-594 for 30 min. Shifting the cells to 37 °C initiated normal transferrin internalization in both mock- and Eps15S ΔEH2/EH3-expressing cells (supplemental Fig. 1, *A* and *B*) but was markedly inhibited in Eps15 ΔEH2/EH3-expressing cells (supplemental Fig. 1*C*) as reported previously (21). Importantly, transferrin was not trafficked to the perinuclear region in Eps15S ΔEH2/EH3-expressing cells following a 20-min chase compared with adjacent nontransfected cells (supplemental Fig. 1, *B′* and *D*). To test if these changes reflected an alteration in TfR recycling back to the cell surface, Clone 9 cells were transfected with either Myc-Eps15S ΔEH2/EH3 or Myc-Eps15 ΔEH2/EH3, and then surface level of TfR during pulse-chase experiment was examined. As observed for the labeled ligand, cells expressing the Eps15S ΔEH2/EH3 exhibited a normal clearance of the TfR upon the pulse (10 min, supplemental Fig. 2*B′*) but were unable to recycle the receptor back to the plasma membrane (chase 40 min, supplemental Fig. 2, *B″* and *D*). These results suggest that Eps15S could mediate recycling of multiple receptors by regulating the integrity of the recycling compartment.

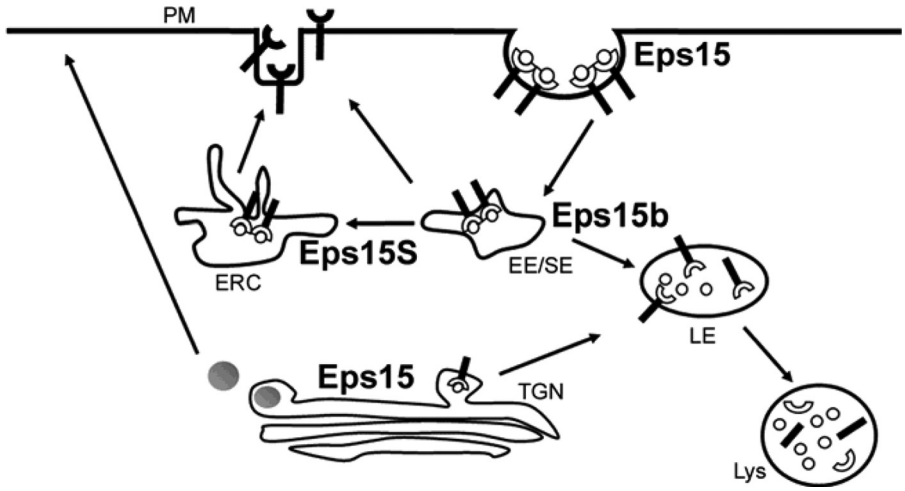

FIGURE 8. **Model depicting roles of three Eps15 forms in EGFR trafficking.** Eps15 functions in internalization of EGFR at the plasma membrane, and Eps15b localized on early endosomes mediates sorting of EGFR to the late endosome/lysosome for degradation. Eps15S directs the internalized EGFR to the recycling endosome for recycling back to the cell surface.

DISCUSSION

Novel Form of Eps15 in Epithelial Cells—In this study we have identified a novel isoform of Eps15 from rat liver termed Eps15S. This novel Eps15 form lacks 111 amino acids of conventional Eps15, including two UIMs at the C terminus that are replaced with three unique residues, and is ubiquitously expressed in brain, liver, spleen, and other tissues. We determined that Eps15S has a unique localization and function compared with the previously characterized forms of Eps15. Eps15S does not localize to early endocytic vesicles like Eps15 or to the early endosome like Eps15b. This observation, together with the fact that Eps15S is missing the C-terminal UIM domains, suggested that this truncated form participates in EGFR recycling rather than degradation. In support of this premise, we found that Eps15S mediates recycling of EGFR. Indeed, overexpression of an Eps15S mutant but not of an Eps15 mutant blocked EGFR recycling. Conversely, following KD of all Eps15 forms, re-expression of Eps15S WT but not Eps15 WT promoted EGFR recycling. Consistent with a function in receptor recycling, overexpression of an Eps15S mutant reduced cell growth. Moreover, Eps15S localized to the Rab11-positive ERC and was required for the localization and structural integrity of this compartment. A mutant Eps15S that blocks EGFR recycling and disrupts positioning of the ERC led to accumulation of the receptor on the early endosome. Taken together, these observations suggest that different Eps15 family members play central roles in directing EGFR toward recycling or degradative pathways.

Eps15S on ERC Mediates EGFR Recycling—A notable characteristic of the Eps15S form compared with the other two variants (Eps15 and Eps15b) is the lack of the C-terminal UIM domains. Eps15 and Eps15b have been suggested to mediate trafficking of ubiquitinated EGFR via these domains and/or an interaction with Hrs (28–32). A central observation of this study is that, in contrast to Eps15 (30, 42), the Eps15S form is not targeted to endocytic vesicles containing ubiquitinated EGFR. Eps15S does not colocalize with rhodamine-labeled EGF even when cells are incubated with 100 ng/ml of this ligand, a sufficiently high concentration to stimulate robust receptor phosphorylation, ubiquitination, and multivesicular bodies (MVB) targeting (7). This finding, combined with the apparent absence of the C-terminal UIM domains in Eps15S, suggests that Eps15 does not participate in the degradative pathway. Instead, the morphological and biochemical studies of Figs. 3–6 indicate participation in the recycling pathway that could affect proliferative and survival signaling. Continuous recycling of the receptor to the cell surface might sustain signaling while reducing receptor degradation. Indeed, overexpression of an Eps15S mutant that inhibited EGFR recycling to the cell surface significantly reduced HeLa cell growth (Fig. 5*E*). Thus, Eps15S may be required not only for short term recycling of the receptor but also for its long term biological function.

Whether Eps15S targets EGFR back to the cell surface via a direct interaction with the receptor tail is currently unclear as we did not observe binding between these two proteins. The Eps15 EH domains support multiple interactions with NPF-containing endocytic adaptor proteins, such as epsin and synaptojanin, at the plasma membrane, and these interactions might also occur at the ERC. Additional interactions with NPF-containing, Rab11-binding proteins such as Rab11-FIP2 and rabenosyn 5, which have been reported to mediate endocytic recycling, may also prove important for Eps15S-mediated EGFR recycling (8, 15, 46).

It was surprising that alterations in Eps15 or Eps15S function, either by mutant expression or siRNA-mediated KD, had only modest effects on EGFR internalization. This finding is somewhat contradictory to a previous report (20) but does mimic the findings of Roxrud *et al.* (32), leaving the function of the conventional Eps15 form somewhat undefined. Stimulating cells with high concentrations of EGF ligand (20–100 ng/ml) activates non-clathrin-based endocytic mechanisms of ubiquitinated EGFR (7, 35) that could be independent of Eps15 function. Indeed, Eps15 ΔEH2/EH3 inhibits the internalization of wild-type EGFR but not of an EGFR mutant fused with ubiquitin (30).

Eps15S Is Required for the Localization and Structural Integrity of the ERC—The hypothesis that Eps15S functions at the ERC is supported further by the localization of this form with Rab11, a classic marker of the ERC. Most striking was the substantial dispersion of the ERC induced by overexpression of the Eps15S ΔEH2/EH3 mutant, whereas expression of the Eps15 mutant had only modest effects. Several explanations could account for this phenomenon. One is that Eps15S functions in receiving EGFR-containing vesicles budded from early endosomes at the recycling endosome. Consistent with this is the accumulation of activated EGFR in the early endosome in cells expressing the Eps15S mutant. Another possibility is that Eps15S functions with microtubule-associated motor proteins as these mechano-enzymes are known to mediate localization of the ERC and transport between endosomes (47). For example, myosin Vb regulates ERC trafficking through a structural interaction with Rab11 via the intermediary Rab11-FIP2 (48–50). In addition, the interaction of sorting nexin 4 (SNX4) with dynein facilitates transport of the transferrin receptor from the early endosome to the ERC and is required for the juxtanuclear positioning of this compartment (51). Determining whether Eps15S forms a functional complex with these or other cytoskeletal components that is disrupted upon mutant expression is a direction we are currently pursuing.

Finally, we found that expression of the Eps15S mutant inhibited transport of internalized transferrin to the perinuclear ERC (supplemental Fig. 1) and subsequently attenuated recycling of the transferrin receptor to the cell surface (supplemental Fig. 2). This is strong evidence that Eps15S is a potent regulator of the ERC and receptor recycling and is not limited to regulation of the EGFR.

In conclusion, this identification of a third Eps15 spliced form suggests that this family of proteins function differentially in EGFR trafficking. Eps15 and Eps15b mediate the internalization and sorting of EGFR to the late endosome/lysosome for degradation, which attenuates cell growth. In contrast, Eps15S directs internalized EGFR to the ERC for transit back to the cell surface, which could enhance growth (Fig. 8).

REFERENCES

1. Maxfield, F. R., and McGraw, T. E. (2004) *Nat. Rev. Mol. Cell Biol.* **5,** 121–132
2. Jones, M. C., Caswell, P. T., and Norman, J. C. (2006) *Curr. Opin. Cell Biol.* **18,** 549–557
3. Doherty, G. J., and McMahon, H. T. (2009) *Annu. Rev. Biochem.* **78,** 857–902
4. Gruenberg, J., and Stenmark, H. (2004) *Nat. Rev. Mol. Cell Biol.* **5,** 317–323
5. Slagsvold, T., Pattni, K., Malerød, L., and Stenmark, H. (2006) *Trends Cell Biol.* **16,** 317–326
6. Woodman, P. G., and Futter, C. E. (2008) *Curr. Opin. Cell Biol.* **20,** 408–414
7. Sigismund, S., Argenzio, E., Tosoni, D., Cavallaro, E., Polo, S., and Di Fiore, P. P. (2008) *Dev. Cell* **15,** 209–219
8. Naslavsky, N., and Caplan, S. (2005) *J. Cell Sci.* **118,** 4093–4101
9. Grant, B. D., and Caplan, S. (2008) *Traffic* **9,** 2043–2052
10. Grant, B. D., and Donaldson, J. G. (2009) *Nat. Rev. Mol. Cell Biol.* **10,** 597–608
11. van der Sluijs, P., Hull, M., Webster, P., Mâle, P., Goud, B., and Mellman, I. (1992) *Cell* **70,** 729–740
12. Sheff, D. R., Daro, E. A., Hull, M., and Mellman, I. (1999) *J. Cell Biol.* **145,** 123–139
13. Kouranti, I., Sachse, M., Arouche, N., Goud, B., and Echard, A. (2006) *Curr. Biol.* **16,** 1719–1725
14. Ren, M., Xu, G., Zeng, J., De Lemos-Chiarandini, C., Adesnik, M., and Sabatini, D. D. (1998) *Proc. Natl. Acad. Sci. U.S.A.* **95,** 6187–6192
15. Naslavsky, N., Rahajeng, J., Sharma, M., Jovic, M., and Caplan, S. (2006) *Mol. Biol. Cell* **17,** 163–177
16. D'Souza-Schorey, C., and Chavrier, P. (2006) *Nat. Rev. Mol. Cell Biol.* **7,** 347–358
17. Sharma, M., Giridharan, S. S., Rahajeng, J., Naslavsky, N., and Caplan, S. (2009) *Mol. Biol. Cell* **20,** 5181–5194
18. Horgan, C. P., and McCaffrey, M. W. (2009) *Biochem. Soc. Trans.* **37,** 1032–1036
19. Carbone, R., Fré, S., Iannolo, G., Belleudi, F., Mancini, P., Pelicci, P. G., Torrisi, M. R., and Di Fiore, P. P. (1997) *Cancer Res.* **57,** 5498–5504
20. Benmerah, A., Bayrou, M., Cerf-Bensussan, N., and Dautry-Varsat, A. (1999) *J. Cell Sci.* **112,** 1303–1311
21. Benmerah, A., Poupon, V., Cerf-Bensussan, N., and Dautry-Varsat, A. (2000) *J. Biol. Chem.* **275,** 3288–3295
22. van Bergen En Henegouwen, P. M. (2009) *Cell Commun. Signal.* **7,** 24
23. Haffner, C., Takei, K., Chen, H., Ringstad, N., Hudson, A., Butler, M. H., Salcini, A. E., Di Fiore, P. P., and De Camilli, P. (1997) *FEBS Lett.* **419,** 175–180
24. Chen, H., Fre, S., Slepnev, V. I., Capua, M. R., Takei, K., Butler, M. H., Di Fiore, P. P., and De Camilli, P. (1998) *Nature* **394,** 793–797
25. Tebar, F., Sorkina, T., Sorkin, A., Ericsson, M., and Kirchhausen, T. (1996) *J. Biol. Chem.* **271,** 28727–28730
26. Iannolo, G., Salcini, A. E., Gaidarov, I., Goodman, O. B., Jr., Baulida, J., Carpenter, G., Pelicci, P. G., Di Fiore, P. P., and Keen, J. H. (1997) *Cancer Res.* **57,** 240–245
27. Klapisz, E., Sorokina, I., Lemeer, S., Pijnenburg, M., Verkleij, A. J., and van Bergen en Henegouwen, P. M. (2002) *J. Biol. Chem.* **277,** 30746–30753
28. Polo, S., Sigismund, S., Faretta, M., Guidi, M., Capua, M. R., Bossi, G., Chen, H., De Camilli, P., and Di Fiore, P. P. (2002) *Nature* **416,** 451–455
29. de Melker, A. A., van der Horst, G., and Borst, J. (2004) *J. Biol. Chem.* **279,** 55465–55473
30. Sigismund, S., Woelk, T., Puri, C., Maspero, E., Tacchetti, C., Transidico, P., Di Fiore, P. P., and Polo, S. (2005) *Proc. Natl. Acad. Sci. U.S.A.* **102,** 2760–2765
31. Hoeller, D., Crosetto, N., Blagoev, B., Raiborg, C., Tikkanen, R., Wagner, S., Kowanetz, K., Breitling, R., Mann, M., Stenmark, H., and Dikic, I. (2006) *Nat. Cell Biol.* **8,** 163–169
32. Roxrud, I., Raiborg, C., Pedersen, N. M., Stang, E., and Stenmark, H. (2008) *J. Cell Biol.* **180,** 1205–1218
33. Cao, H., Weller, S., Orth, J. D., Chen, J., Huang, B., Chen, J. L., Stamnes, M., and McNiven, M. A. (2005) *Nat. Cell Biol.* **7,** 483–492
34. Chi, S., Cao, H., Chen, J., and McNiven, M. A. (2008) *Mol. Biol. Cell* **19,** 3564–3575
35. Orth, J. D., Krueger, E. W., Weller, S. G., and McNiven, M. A. (2006) *Cancer Res.* **66,** 3603–3610
36. Cao, H., Chen, J., Krueger, E. W., and McNiven, M. A. (2010) *Mol. Cell. Biol.* **30,** 781–792
37. Henley, J. R., Krueger, E. W., Oswald, B. J., and McNiven, M. A. (1998) *J. Cell Biol.* **141,** 85–99
38. Fazioli, F., Minichiello, L., Matoskova, B., Wong, W. T., and Di Fiore, P. P. (1993) *Mol. Cell. Biol.* **13,** 5814–5828
39. Bache, K. G., Raiborg, C., Mehlum, A., and Stenmark, H. (2003) *J. Biol. Chem.* **278,** 12513–12521
40. Coda, L., Salcini, A. E., Confalonieri, S., Pelicci, G., Sorkina, T., Sorkin, A., Pelicci, P. G., and Di Fiore, P. P. (1998) *J. Biol. Chem.* **273,** 3003–3012
41. Poupon, V., Polo, S., Vecchi, M., Martin, G., Dautry-Varsat, A., Cerf-Bensussan, N., Di Fiore, P. P., and Benmerah, A. (2002) *J. Biol. Chem.* **277,** 8941–8948
42. Torrisi, M. R., Lotti, L. V., Belleudi, F., Gradini, R., Salcini, A. E., Confalonieri, S., Pelicci, P. G., and Di Fiore, P. P. (1999) *Mol. Biol. Cell* **10,** 417–434

43. Acconcia, F., Sigismund, S., and Polo, S. (2009) *Exp. Cell Res.* **315,** 1610–1618
44. Ullrich, O., Reinsch, S., Urbé, S., Zerial, M., and Parton, R. G. (1996) *J. Cell Biol.* **135,** 913–924
45. Schlierf, B., Fey, G. H., Hauber, J., Hocke, G. M., and Rosorius, O. (2000) *Exp. Cell Res.* **259,** 257–265
46. Naslavsky, N., Boehm, M., Backlund, P. S., Jr., and Caplan, S. (2004) *Mol. Biol. Cell* **15,** 2410–2422
47. Soldati, T., and Schliwa, M. (2006) *Nat. Rev. Mol. Cell Biol.* **7,** 897–908
48. Nedvetsky, P. I., Stefan, E., Frische, S., Santamaria, K., Wiesner, B., Valenti, G., Hammer, J. A., 3rd, Nielsen, S., Goldenring, J. R., Rosenthal, W., and Klussmann, E. (2007) *Traffic* **8,** 110–123
49. Swiatecka-Urban, A., Talebian, L., Kanno, E., Moreau-Marquis, S., Coutermarsh, B., Hansen, K., Karlson, K. H., Barnaby, R., Cheney, R. E., Langford, G. M., Fukuda, M., and Stanton, B. A. (2007) *J. Biol. Chem.* **282,** 23725–23736
50. Wang, Z., Edwards, J. G., Riley, N., Provance, D. W., Jr., Karcher, R., Li, X. D., Davison, I. G., Ikebe, M., Mercer, J. A., Kauer, J. A., and Ehlers, M. D. (2008) *Cell* **135,** 535–548
51. Traer, C. J., Rutherford, A. C., Palmer, K. J., Wassmer, T., Oakley, J., Attar, N., Carlton, J. G., Kremerskothen, J., Stephens, D. J., and Cullen, P. J. (2007) *Nat. Cell Biol.* **9,** 1370–1380